New Asymmetric [CuATSM] Analogues for Neurodegeneration Diagnosis and Therapy: Donor Atom Effects on Redox Potential and Reversibility

Alexis Joannidis

Bio21 Molecular Science and Biotechnology Institute, The University of Melbourne, Parkville, Melbourne, 3010, Australia

Summary for Public Release: [*CuATSM] is a copper-based compound undergoing clinical trials for Parkinson's disease and MND, with potential for the diagnosis and treatment of these and Alzheimer's disease. Next generation variants, focused on two of its proposed mechanisms of action were developed, with the aim of improving understanding and/or efficacy of its activity.*

Introduction

Copper (diacetyl-bis(4-methyl-3-thiosemicarbazone)) [CuATSM] (fig. 1) is a charge neutral, lipophilic, blood-brain-barrier permeable, square planar complex with potential implications for the treatment and diagnosis of neurological degenerative diseases including Parkinson's Disease (PD)[1], Alzheimer's Disease (AD)[2] and Amyotrophic Lateral Sclerosis (ALS)[3]. Its diagnostic potential arises from its ability to be radiolabeled with copper-64, a radioactive isotope with a 12.7 h half-life, coupled with the possibility of appending functional groups that bind to compounds in the brain implicated with neurological disease[4].

Its therapeutic potential is multifaceted, and is not fully understood, though its biological activity can in part be attributed to the $Cu^{II/I}$ reduction potential, allowing for the reduction of Cu^{II} to Cu^{I} in the reducing environment of the cell. This facilitates the transfer of Cu from the complex to high-affinity copper binding metalloproteins, some of which are implicated in disease, such as SOD-1 in ALS[3].

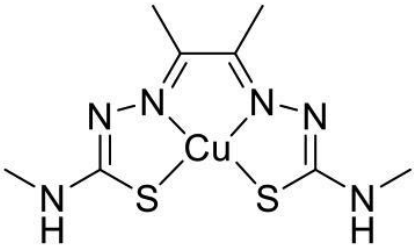

Figure 1. [CuATSM]

The reversibility of the corresponding reduction/oxidation cycle is dependent on the distortion of the complex that may arise from the change in geometry dictated by the copper redox state, and also upon the affinity of the ligand donor atoms for reduced Cu^{I}. [CuATSM] is unusual in its high redox reversibility, but it is unclear whether this is important to its biological function.

Varying the reversibility of Cu(thiosemicarbazonato) complexes is therefore of interest in determining how these chemical effects translate to biological activity.

In this project we changed the donor atoms of such ligands to observe their effect on the reducibility of the Cu^{II}/Cu^{I} redox cycle, to probe whether such modifications are a viable route for the development of metal complexes with poorer reversibility. Such compounds may then be used to determine the importance of reducibility on biological activity.

The functionality of the rest of the complex is also of interest for therapeutic activity. Ferroptosis is a recently characterized pathway of cell death implicated in ALS, PD and AD. It is characterized by iron-dependent lipid peroxidation, and [CuATSM] exhibits antiferroptotic behaviour by preventing lipid radical propagation[5]. It is hypothesized that this is due to potential H-atom donor sites on the N*H*-CH_3 groups; the resulting radical is stabilized by delocalization over the conjugated ligand backbone, and the donated H quenches radical propagation.

To this end, we synthesized and characterized several asymmetric M^{II}(thiosemicarbazonato) complexes with varied H-atom donor sites.

Results and Discussion

Mono-ketone thiosemicarbazones (1-3) were prepared by a literature procedure (scheme 1).

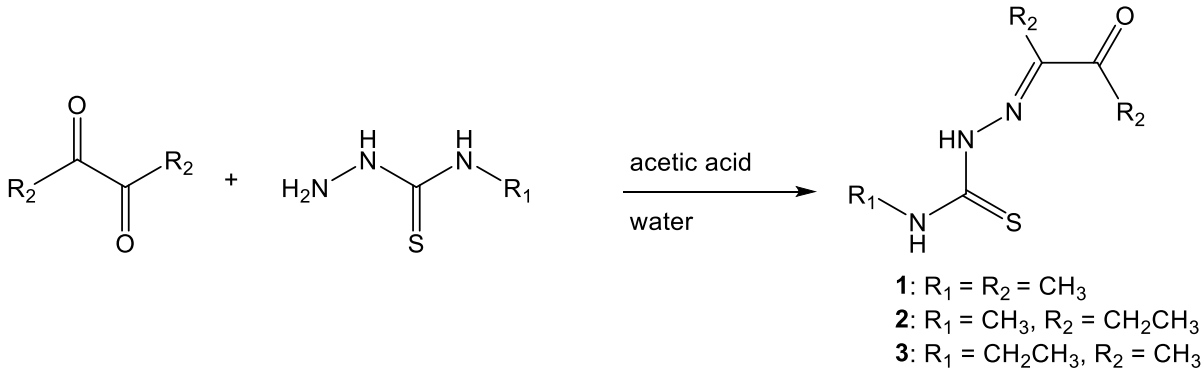

Scheme 1. Small molecule synthesis of **1-3**

The non-symmetrical analogues ($H_2\mathbf{L^1}$-$H_2\mathbf{L^3}$) were prepared by reacting 1,2 and 3 with aminoguanidine bicarbonate (scheme 2). This was attempted first in DMF at room temperature overnight but the ease of synthesis using ethanol at reflux was the preferred method, though it was not able to reliably yield the correct product ($H_2\mathbf{L^2}$, $H_2\mathbf{L^3}$, $H_2\mathbf{L^4}$) after subsequent attempts with **2, 3**.

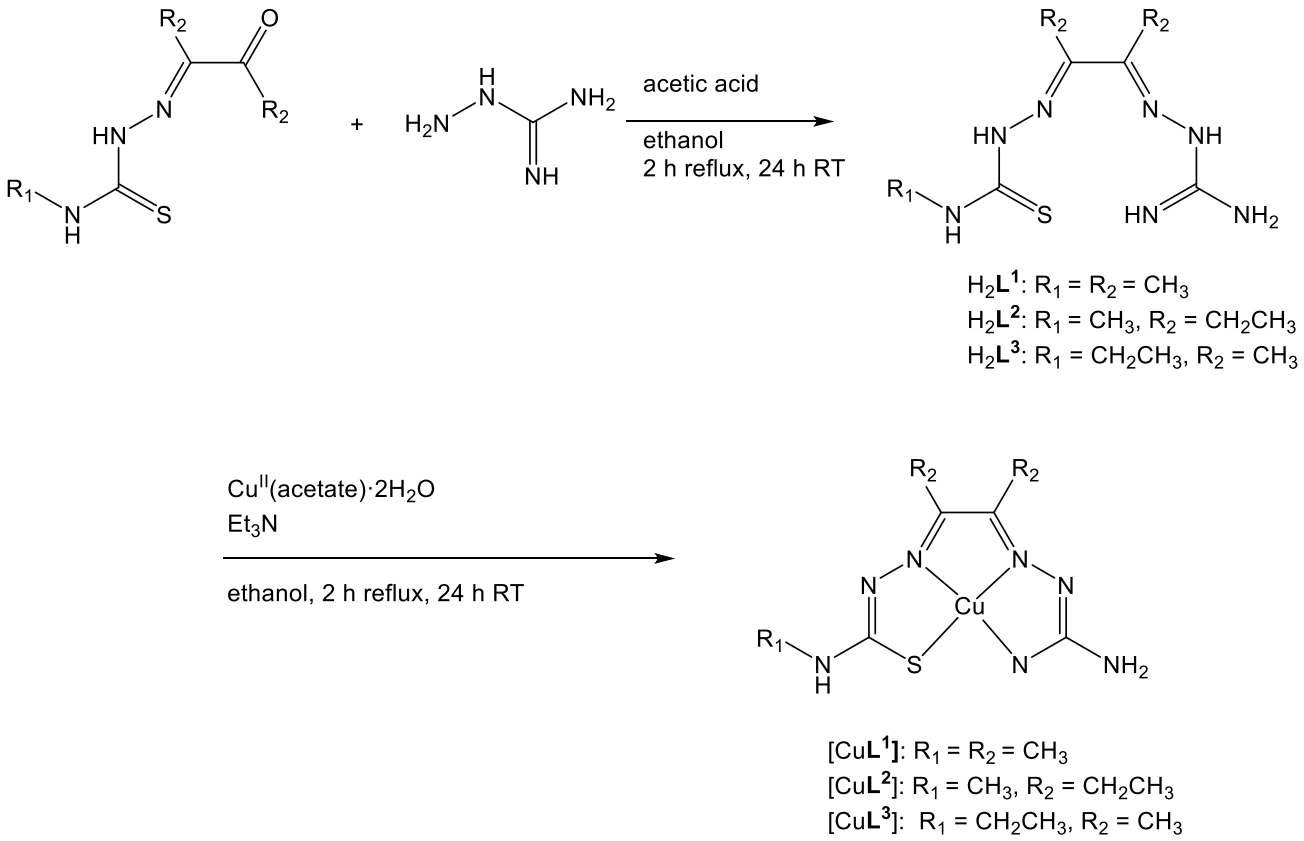

Scheme 2. Aminoguanidine ligand and complex synthesis

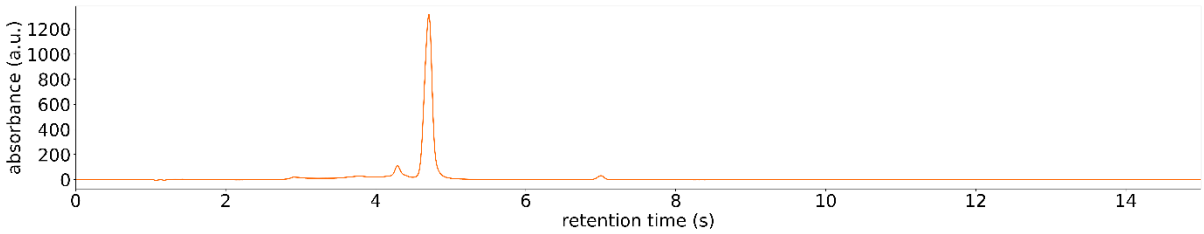

Figure 2. $H_2\mathbf{L^1}$ HPLC chromatogram, UV detection (λ_{abs} = 254 nm)

Owing to phenylsemicarbazide's poor solubility the phenylsemicarbazide ligands could not be synthesized using the same procedure as $H_2\mathbf{L^1}$; the reaction was only successful in DMF under a N_2 environment.

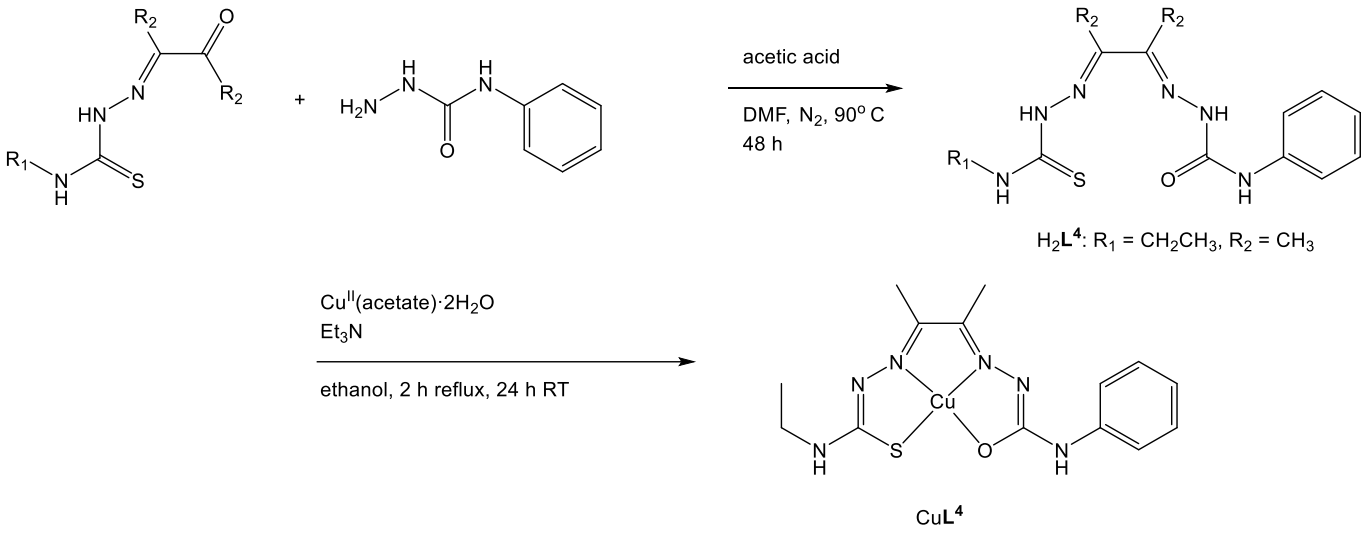

Scheme 3. 4-phenylsemicarbazide ligand and complex synthesis

The aminated rings, o-phenylenediamine and 3,4-diaminobenzoic acid initially proved difficult to work with. An attempt to form H_2**L**^{5} in ethanol in fact yielded H_2ATSM as characterized by ESI-MS and ^{1}H-NMR (Appendix 2: Fig. 24). We posit that this is attributed to nucleophilic catalytic activity of o-phenylenediamine, following the same mechanism as has been previously observed for aniline and several of its derivatives[7].

The eventual synthesis of Ni**L**^{5} was completed via a template reaction, several variations of which were attempted by changing the order in which the starting materials were added to nickel^{II}(acetate) tetrahydrate, though the variation reported yielded the highest purity according to ESI-MS and HPLC.

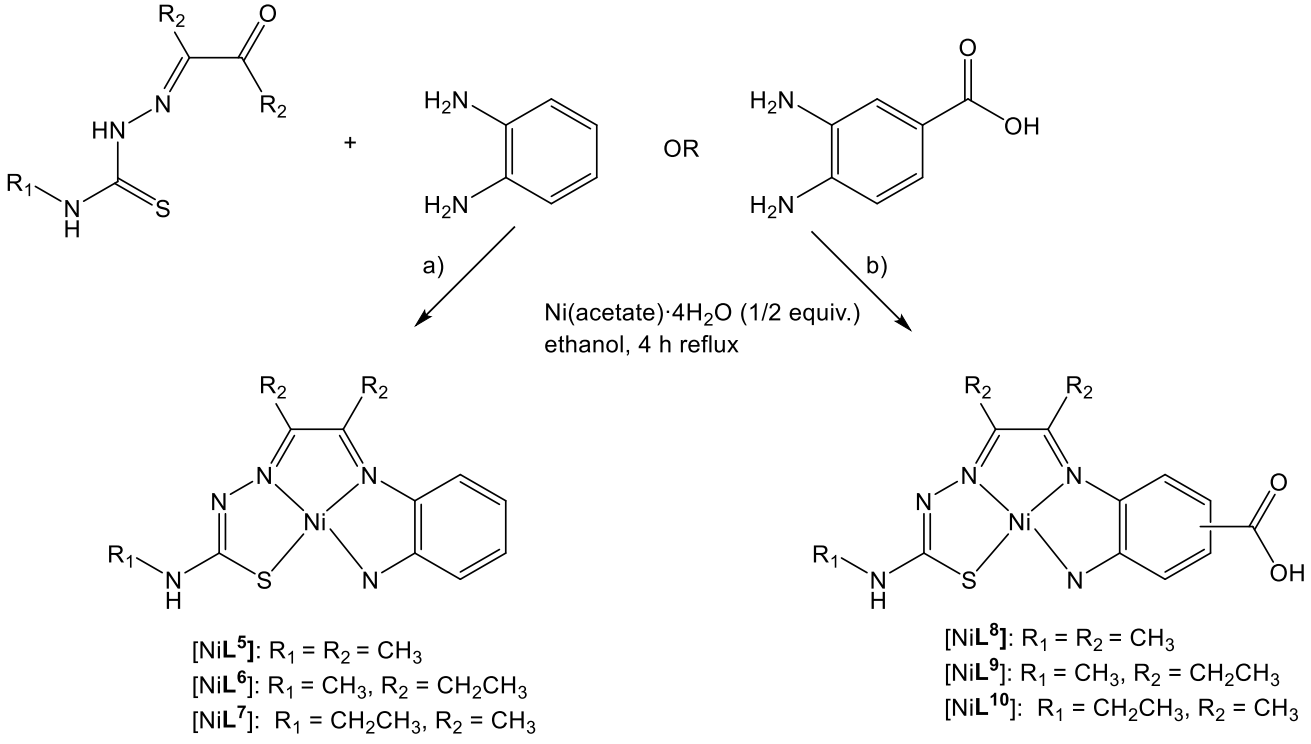

Scheme 4. nickle template effect complex synthesis

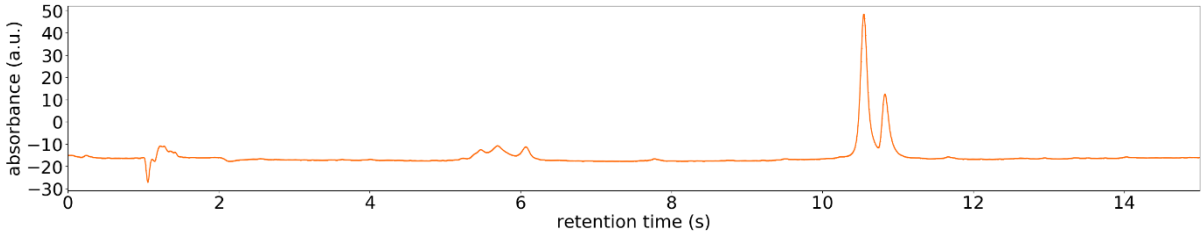

Figure 3. Ni**L**^{5} HPLC chromatogram, UV detection (λ_{abs} = 254 nm)

These complexes were formed using nickel instead of copper, as the desired square planar geometry results in paramagnetic Cu^{II} which cannot be analyzed by NMR, in contrast to the diamagnetic Ni^{II}. The template reactions were initially conducted using Ni(acetate) tetrahydrate, though ^{1}H NMR analysis of the resultant complexes indicated that these were in fact paramagnetic complexes. It was hypothesized that acetate forms axial interactions with the Ni^{II} of the desired square planar complex, tending towards an octahedral geometry resulting in paramagnetic Ni^{II}.

Attempts were made to extract the metal from the complex to allow analysis of the free ligand. An EDTA chelation of Ni was attempted first, but the small scale used made any product difficult to collect so the method was not pursued. An attempt to protonate the ligand and remove the metal from the complex via a solvent separation (water/diethyl ether) was made, but the ligand was not identified in either solvent fraction, potentially indicating it was decomposed by HCl in the process.

Failing these methods, Ni**L**^{5} was again synthesized, using $NiBF_4$ with the intent that the poorer BF_4 ligand would not exhibit the same axial interactions as acetate. ^{1}H-NMR indicated a diamagnetic compound was synthesized, though F-NMR showed a single peak (δ_F = -70 ppm). This is possibly explained by the presence of F^- as a counter anion, or by an axial interaction leading to a square-pyramidal geometry which retains diamagnetism. X-ray crystallography may be used to determine the nature of this F presence.

UV-Vis spectroscopy allowed identification of metal-ligand charge transfer bands for complexes of both metals (λ = 400-600 nm), which were absent from H_2**L**^{4} (fig. 4, 5). These large peaks were deemed charge-transfer bands as their high absorbance indicated high extinction coefficients associated with allowed transitions, and not from spin-forbidden metal d-d electronc transitions. $\pi - \pi^*$ transitions within the ligands were also identified (λ < 400 nm).

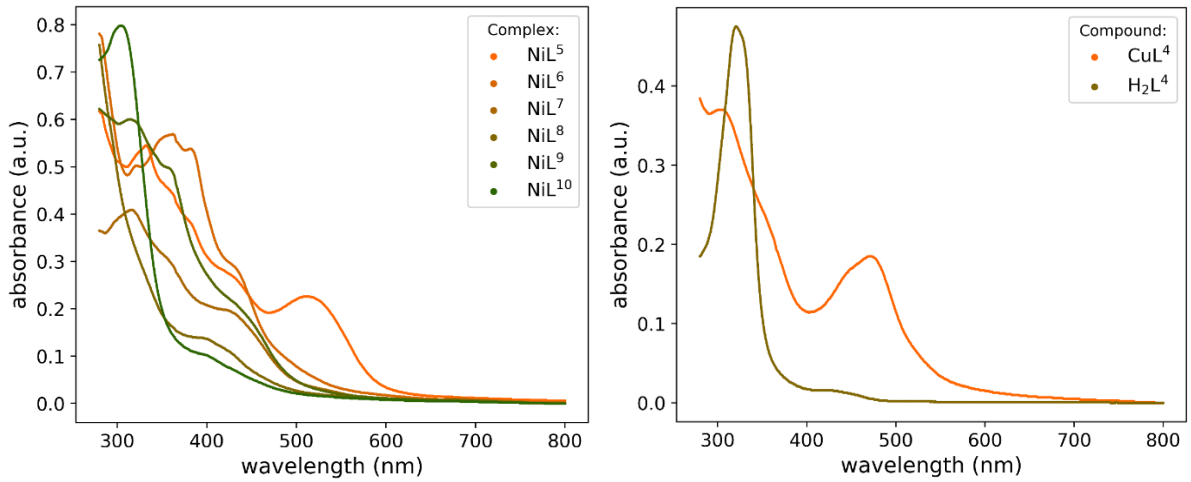

Figures 4, 5. UV-Vis absorbance spectra for Ni^{II} complexes (left), and comparison for Cu**L**^{4} and ligand H_2**L**^{4}

Though [CuATSM]'s biological activity is in many ways unclear, its function can be partly attributed to its reduction from Cu^{II} to Cu^{I} in the cell. Cu^{II} is a borderline hard/soft acid with stronger affinity for intermediate/hard bases, while Cu^{I} is a soft acid with preference for soft bases. Hence, the reduction of the complex will change the affinity of copper towards the ligand's donor atoms, depending on their hardness. [CuATSM] binds copper to soft sulfur, so the reduction to Cu^{I} is favourable due to the higher metal-ligand affinity.

The effect of donor atom hardness was probed by cyclic voltammetry. Cu**L**^{1} replaces one of the [CuATSM] S donor atoms for harder N. The lower affinity after reduction makes the reduction less favourable and so a stronger reducing potential is required than for [CuATSM] (E^{o}' = -1.13 V)[6] (table 1).

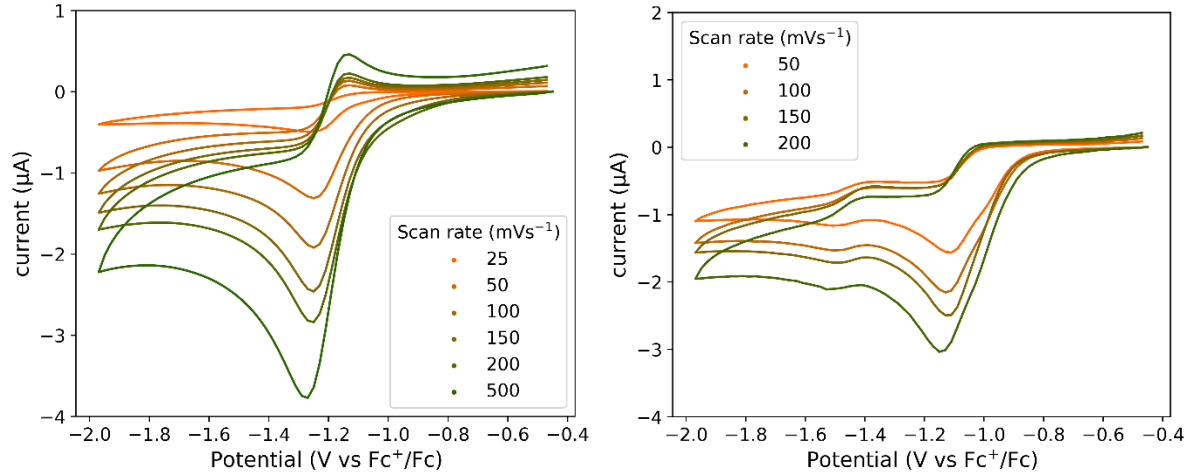

Figure 6, 7. Cyclic voltammograms of [Cu**L**^{1}] (left), [Cu**L**^{4}] in dimethylformamide at a glassy carbon working electrode, 1 mmol L^{-1} analyte, electrolyte = 0.1 mol L^{-1} tetrabutylammonium hexafluorophosphate. Potentials quoted versus Fc+ /Fc. Clockwise scanning direction.

Table 1. Summary of the $Cu^{II/I}$ Reduction Potentials

compound	$E^{o'}$ ($Cu^{II/I}$) (vs Fc^{+}/Fc)	I_c/I_a	peak separation (mV)
CuL^1	-1.19	3.14	62
CuL^4	-1.16	20.6	80

[CuATSM] is unusual in that it is quasi-reversible. Cu**L**$^{\mathbf{1}}$ and Cu**L**$^{\mathbf{4}}$ were notably less reversible, showing deviation from the 59 mV peak separation of an ideal reversible single electron process, and with large I_c/I_a values (fig. 6, 7, table 1). This is potentially due to the lower affinity of Cu^I for these hard donor atoms causing an irreversible degradation of the complex, or to the preference of Cu^I for tetrahedral geometry causing a geometric shift and irreversible distortion to the ligands. It is unclear whether the reversibility of [CuATSM] is crucial to its biological function; Therefore, evidence that donor atom hardness impacts the redox reversibility suggests an avenue for developing molecules with lessened reversibility to determine the biological importance of this attribute.

The H-atom donor potential of Cu(thiosemicarbazonato) complexes is thought to be implicated in their antiferroptotic behaviour. The aminoguanidine and 4-phenylsemicarbazide derived complexes contain potential amine H-atom donors, and a conjugated ligand backbone capable of delocalized stabilization of the resultant radical, favoring their donor activity. The aromatic amine complexes (o-phenylenediamine and 3,4-diaminobenzoic acid derived) lack these features once complexed, but gain them in the metal-free ligand forms. Hence, it may be of interest to further probe the antiferroptotic potential of these Cu(thiosemicarbazonato) complexes, and to determine whether the H-atom donor capacity of the metal-free ligands is of relevance, once Cu^{II} is reduced and extracted from the complexes in the cell environment.

Conclusion

Various asymmetric Cu(thiosemicarbazonato) and Ni(thiosemicarbazonato) complexes were synthesized and characterized, allowing for variations of both donor atoms and H-atom donor sites. Redox activities of the complexes were probed by cyclic voltammetry, indicating that reduction potential and reversibility is influenced by the relative affinities of the donor atoms to Cu^{II} and reduced Cu^{I}.

Experimental Section

General Procedures. NMR spectra were recorded on a Varian FT-500 NMR (California, USA) (^{1}H at 500 MHz and ^{13}C{^{1}H} at 125.7 MHz) at 297 K and referenced to internal solvent residue. High resolution mass spectra were recorded on a Thermo Scientific Exactive Plus OrbiTrap LC/MS (Thermo Fisher Scientific, Massachusetts, USA) and calibrated to internal references. Analytical RP-HPLC traces were acquired using an Agilent 1200 HPLC system equipped with an Phenomenex Kinetex EVO C18 Analytical HPLC column (4.6 x 100 mm, 5 μm) with a flow rate of 1 mL/min and UV absorbance detection at 254 nm. Retention times (Rt /min) were recorded using a gradient elution of 5−100% B in A (A = 0.1% trifluoroacetic acid (TFA), B = acetonitrile with 0.1% TFA) over 30 min. UV−vis spectra were recorded on a Shimadzu UV1650-PC spectrometer (Shimadzu, Kyoto, Japan) from 800 to 280 nm.

Cyclic voltammograms were recorded using an Metrohm (Switzerland) AUTOLAB PGSTAT100 and analyzed using Autolab GPES V4.9 software. Measurements were carried out using 1 mM of analyte in anhydrous DMF with tetrabutylammonium hexafluorophosphate (0.1 M) as a supporting electrolyte. A glassy carbon working electrode was used along with a Pt wire counter electrode and a pseudo leakless Ag/Ag+ working electrode (EDAQ, New South Wales, Australia). Measurements were referenced to internal ferrocene (Fc/Fc+ , $E^{\circ\prime} = 0.00$ V where E′ refers to the midpoint of the reduction (Epc) and oxidation (Epa) peaks of a quasi- or fully reversible process where E′ = (Epc + Epa)/2.

Small Molecule Synthesis. Diacetyl-mono-4-methyl-3-thiosemicarbazone, 1. This compound was produced by a previously reported procedure[6]. A solution of 2,3-butanedione (1.20 g, 13.9 mmol) in distilled water (25 mL) was acidified with a few drops of conc. HCl (36%) and cooled to 5° C. 4-methyl-3-thiosemicarbazide (2.65 g, 25.2 mmol) was added incrementally to the stirred cold solution over 1.5 h to produce a white precipitate which was stirred for 40 minutes further. The precipitate was extracted into chloroform (25 + 25 + 20 mL) and the organic extracts were combined, dried over $MgSO_4$, filtered and concentrated. N-pentane was added to the solution until turbidity and it was cooled on ice to give white needles. The product was collected by filtration, washed with *N*-pentane and dried to give **1** (1.43 g, 65%). ^{1}H NMR (d_6-DMSO, 500 MHz): δ = 1.96, 3H, s, CH_3; 2.42, 3H, s, CH_3; 3.05, 3H, d, NH-CH_3; 8.62, 1H, m, NH; 10.61, 1H, s, NH. ESI-MS: (+ve ion) m/z 100% [M+H$^+$] 174.07.

2. Following the same procedure for the synthesis of **1**, using 3,4-hexanedione (1.58 mL, 13.0 mmol) and 4-methyl-3-thiosemicarbazide (2.65 g, 25.2 mmol,) yielded off-white crystals (1.57 g, 62%). ^{1}H NMR (d_6-DMSO, 500 MHz): δ = 0.85, 3H, t, CH_3; 0.97, 3H, t, CH_3; 2.57, 2H, q, CH_2; 2.95, 2H, q, CH_2; ,3.05, 3H, d, NH-CH_3; 8.57, 1H, m, NH; 10.84, 1H, s, NH. ESI-MS: (+ve ion) m/z 100% [M+H$^+$] 257.14.

3. Following the same procedure for the synthesis of **1**, using 2,3-butanedione (1.20 g, 13.9 mmol) and 4-ethyl-3-thiosemicarbazone (1.55 g, 13.0 mmol), yielded off white crystals (1.81 g, 9.65 mmol, 74%). ^{1}H NMR (d_6-DMSO, 500 MHz): δ = 1.15, 3H, s, CH_3; 1.95, 3H, s, CH_3; 2.42, 3H, s, CH_3; 3.62, 2H, q, CH_2; 8.66, 1H, m, NH; 10.56, 1H, s, NH. ESI-MS: (+ve ion) m/z 100% [M+H$^+$] 174.07.

Ligand Synthesis. H_2L^1. To a solution of **1** (150 mg, 0.866 mmol) in ethanol (11 mL) was added aminoguanidine bicarbonate (141 mg, 1.04 mmol) and 10 drops glacial acetic acid, and the solution was heated at reflux for 2 h. The resultant yellow solution was left at 25° C for 24 h, concentrated and a slight yellow precipitate was formed by adding water (25 mL) and cooling on ice. The precipitate was collected by filtration, and washed in H_2O and diethyl ether, yielding translucent off-white flakes (93.9 mg, 0.411 mmol, 47%). ESI-MS: (+ve ion) m/z 100% $[M+H^+]$ 230.1179.

H_2L^4. To a solution of **3** (74.9 mg, 0.400 mmol) in dry DMF acidified with 6 drops glacial acetic acid was added 4-phenyl-semicarbazide (60.47 mg, 0.400 mmol). The solution was stirred at 90° C for 72 h under a N_2 atmosphere. The resultant yellow solution was chilled to 5° C affording a granular precipitate, which was further precipitated with water, collected by filtration and washed with diethyl ether to yield a yellow powder (24.4 mg, 0.0762 mmol, 19 %). ESI-MS: (+ve ion) m/z 100% $[M+H^+]$ 321.1492.

Complex formation. CuL^1. To a solution of $H_2\mathbf{L^1}$ (91.6 mg, 0.4 mmol) in ethanol and 6 drops triethylamine was added Cu^{II}(acetate) dihydrate (79.9 mg, 0.4 mmol). The solution immediately turned a deep brown and was heated to reflux at 90° C for 2 h, and left at room temperature for a further 24 h. A dark precipitate had formed by this point, was concentrated and precipitated upon addition of 15 mL water. The precipitate was collected by filtration and washed with water followed by diethyl ether to yield a deep purple/black powder (74.3 mg, 0.256 mmol, 64 %). ESI-MS: (+ve ion) m/z 100% $[M+2H^+ z = 2]$ 144.9822.

CuL^4: Same procedure as previous, replacing $H_2\mathbf{L^1}$ with $H_2\mathbf{L^4}$ to yield a brown precipitate (58.4 mg, 0.153 mmol, 51%). ESI-MS: (+ve ion) m/z 100% $[M+H^+]$ 382.0630.

NiL^5. A solution of $Ni^{II}(BF_4)$ (510 mg, 1.5 mmol) and o-phenylenediamine (324 mg, 3.0 mmol) in ethanol (10 mL) was heated to reflux for 2 h and left at room temperature for 24 h. At this point the solution was deep bottle green and was acidified with 6 drops glacial acetic acid. Upon addition of **1 (**520 mg, 3.0 mmol), the solution quickly became maroon, and was heated to reflux for a further 2 h. A precipitate had formed and was concentrated under reduced pressure. Water (15 mL) was added and the mixture was chilled to 5° C, collected by filtration and washed with water and diethyl ether, yielding maroon powder (409 mg, 2.55 mmol, 85 %). ESI-MS: (+ve ion) m/z 100% $[M+2H^+ z = 2]$ 159.0917, m/z 100% $[M+H^+ z = 1]$ 317.0147.

NiL^{6-9}. Same as previous, except Ni^{II}(acetate) tetrahydrate instead of $Ni^{II}(BF_4)$ hexahydrate. (81-91 %).

References

1. Hung, L. W., Villemagne, V. L., Cheng, L., Sherratt, N. A., Ayton, S., White, A. R., Crouch, P. J., Lim, S., Leong, S. L., Wilkins, S., George, J., Roberts, B. R., Pham, C. L., Liu, X., Chiu, F. C., Shackleford, D. M., Powell, A. K., Masters, C. L., Bush, A. I., O'Keefe, G., … Barnham, K. J. (2012). The Journal of experimental medicine, 209(4), 837–854.

2. Choo, X., Liddell, J., Huuskonen, M., Grubman, A., Moujalled, D., Roberts, J., Kysenius, K., Patten, L., Quek, H., Oikari, L., Duncan, C., James, S., McInnes, L., Hayne, D., Donnelly, P., Pollari, E., Vähätalo, S., Lejavová, K., Kettunen, M., Malm, T., Koistinaho, J., White, A., & Kanninen, K. (2018). Frontiers in Neuroscience, 12, 668.

3. Nikseresht, S., Hilton, J. B., Kysenius, K., Liddell, J. R. & Crouch, P. J. (2020). Copper-ATSM as a Treatment for ALS: Support from Mutant SOD1 Models and Beyond. Life, 10(11), pp. 14-. doi:10.3390/life10110271

4. Lim, S., Paterson, B., Fodero-Tavoletti, M., O'Keefe, G., Cappai, R., Barnham, K., Villemagne, V., & Donnelly, P. (2010). Chem. Commun., 46, 5437-5439.

5. Southon, A., Szostak, K., Acevedo, K. M., Dent, K. A., Volitakis, I., Belaidi, A. A., Barnham, K. J., Crouch, P. J., Ayton, S., Donnelly, P. S., & Bush, A. I. (2020). British journal of pharmacology, 177(3), 656–667.

6. Paterson, B. M., Karas, J. A., Scanlon, D. B., White, J. M., & Donnelly, P. S. (2010). Inorganic chemistry, 49(4), 1884–1893.

7. Cordes, E., & Jencks, W. (1962). Journal of the American Chemical Society, 84(5), 826-831.

Appendix 1: ESI-MS spectra

Mono ketones

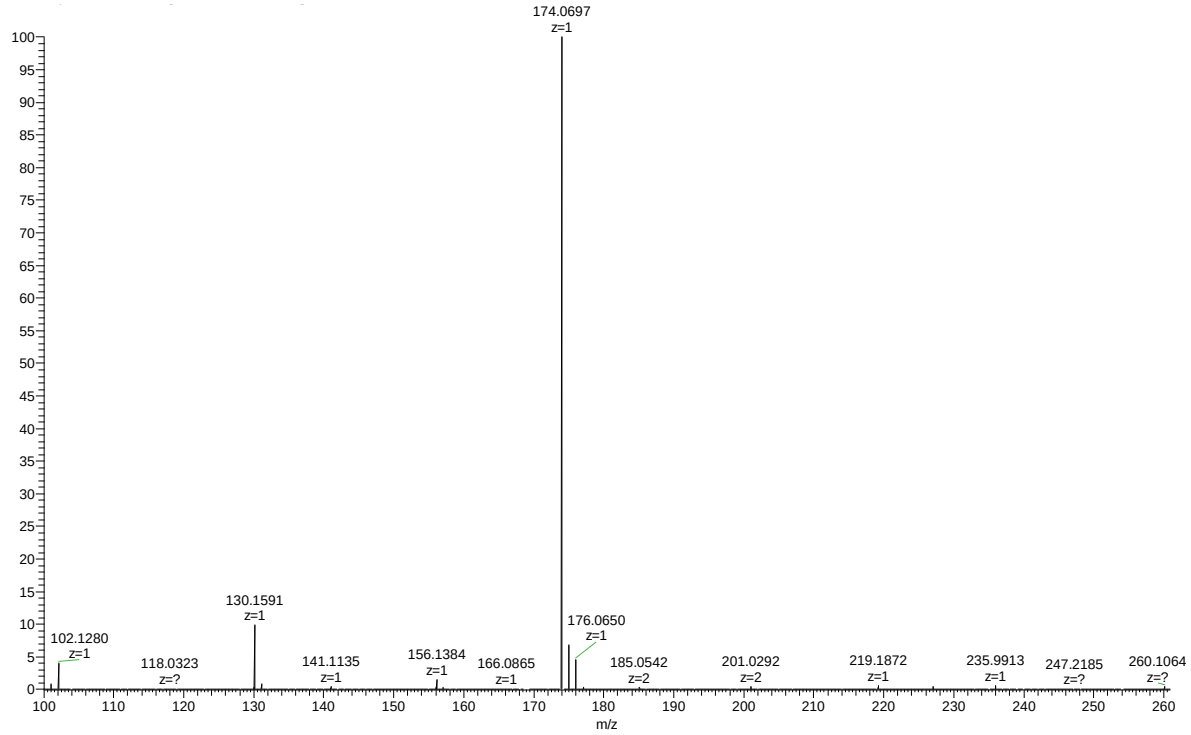

Fig 8. ESI-MS spectra of **1**

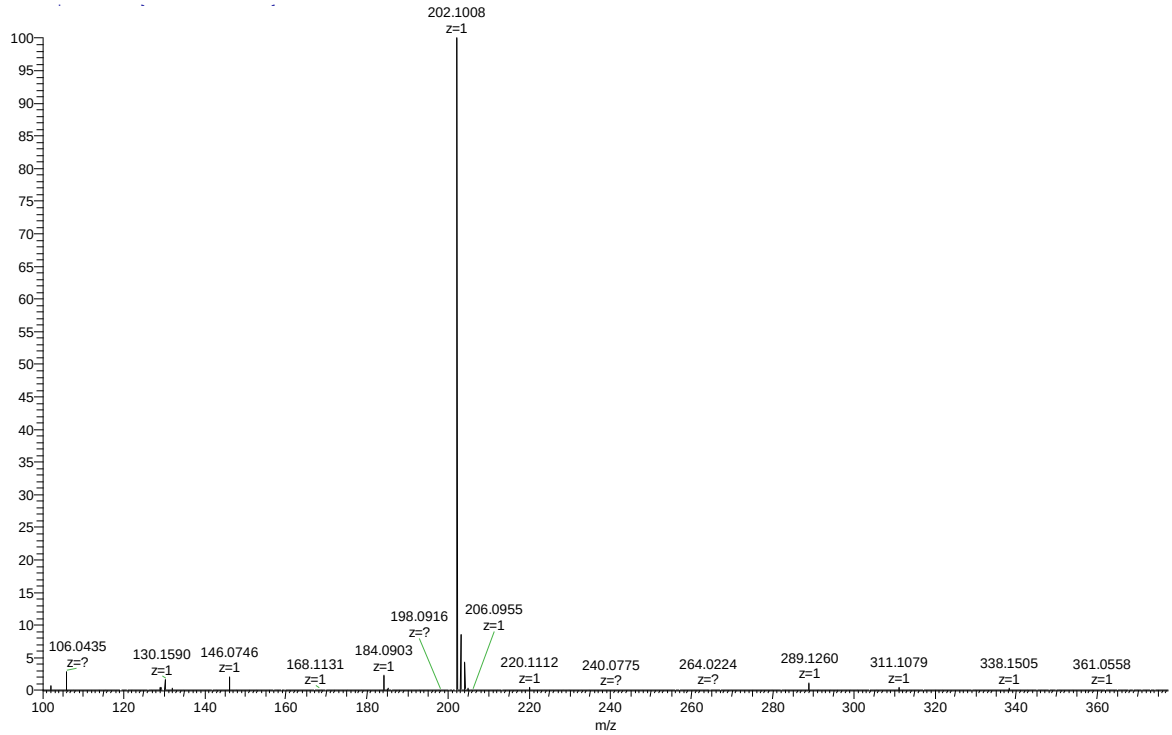

Fig 9. ESI-MS spectra of **2**

Ligands

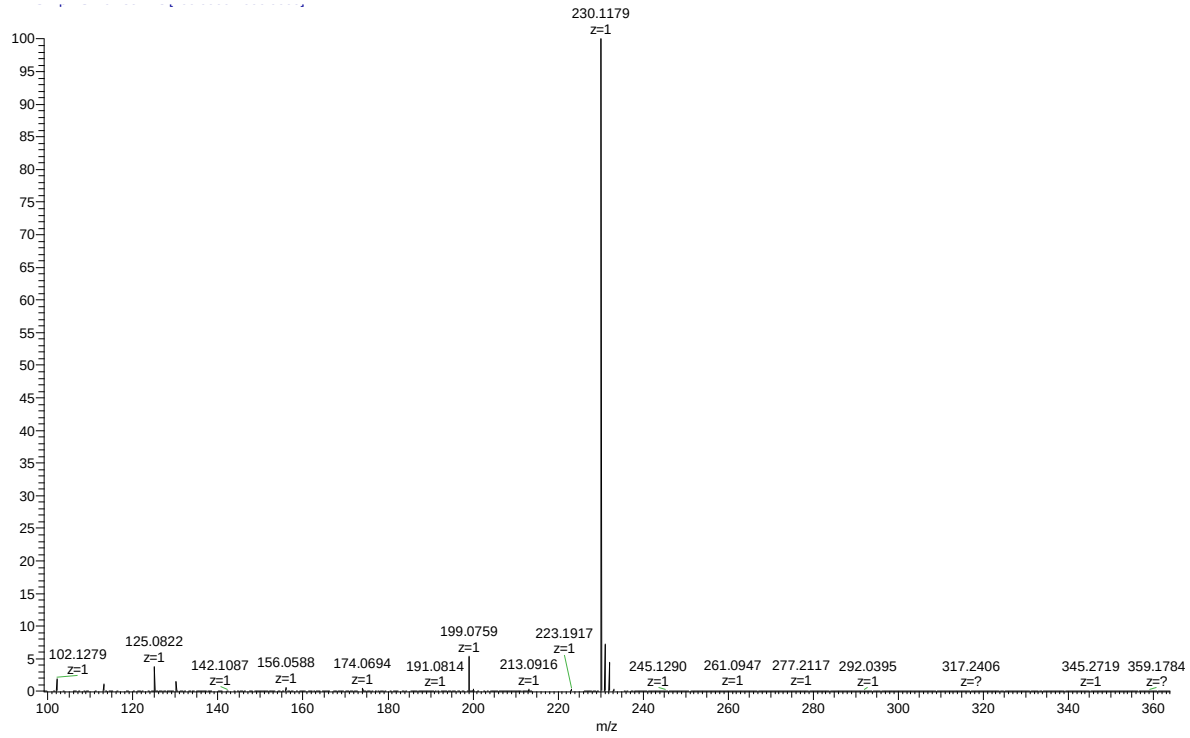

Fig 8. ESI-MS spectra of $H_2\mathbf{L}^1$

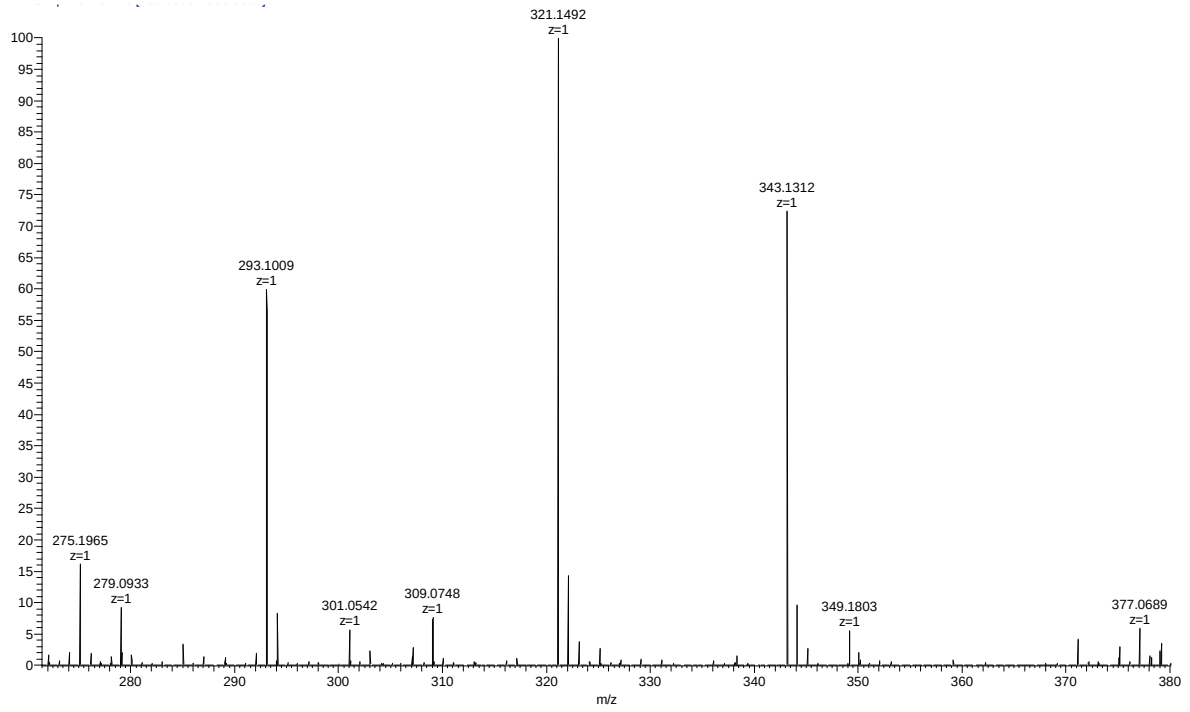

Fig 9. ESI-MS spectra of $H_2\mathbf{L}^4$

Complexes

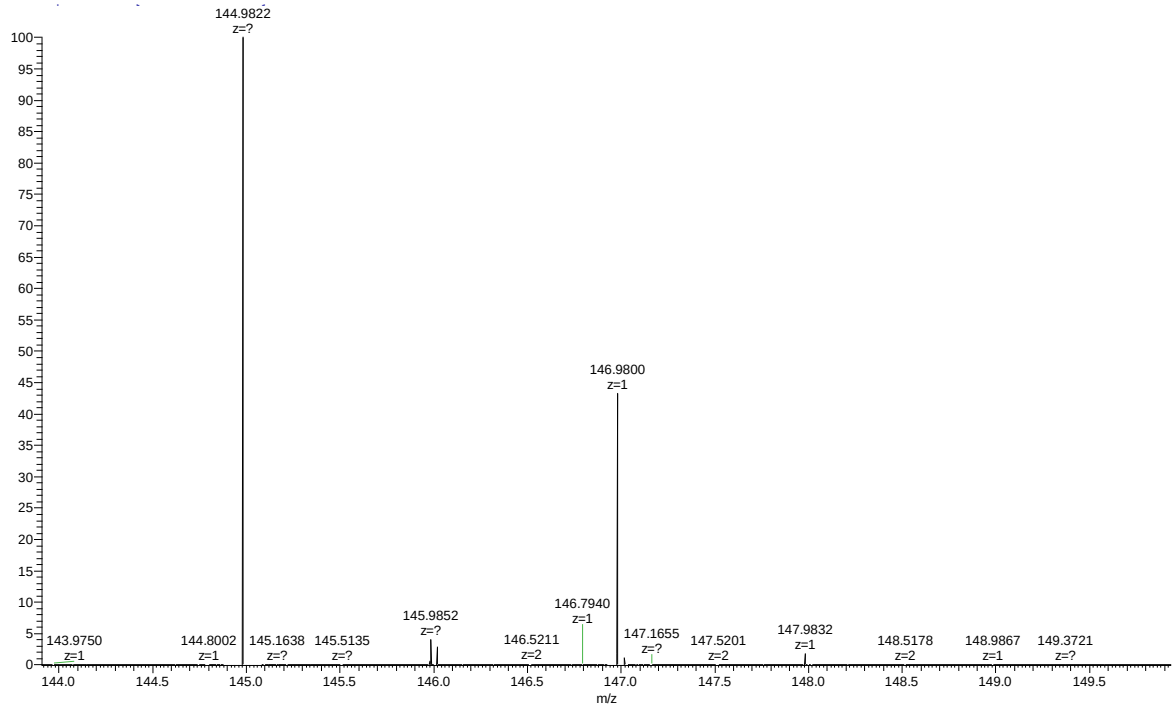

Fig 10. ESI-MS spectra of Cu**L**[1]

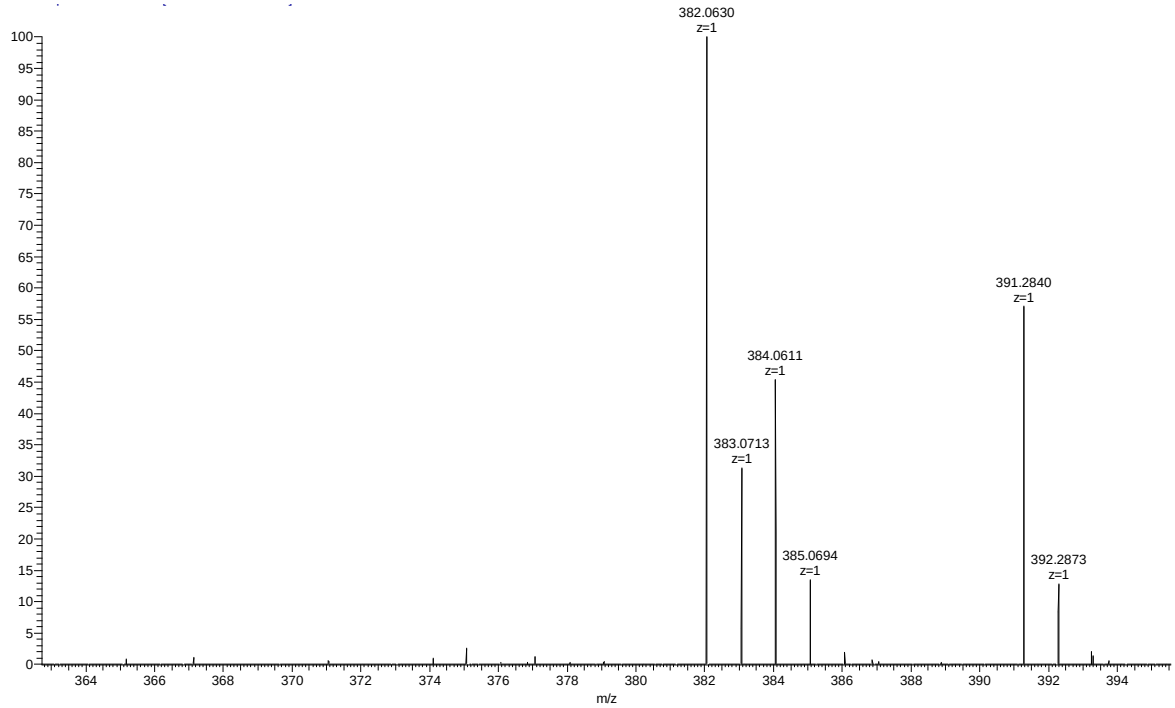

Fig 11. ESI-MS spectra of Cu**L**[4]

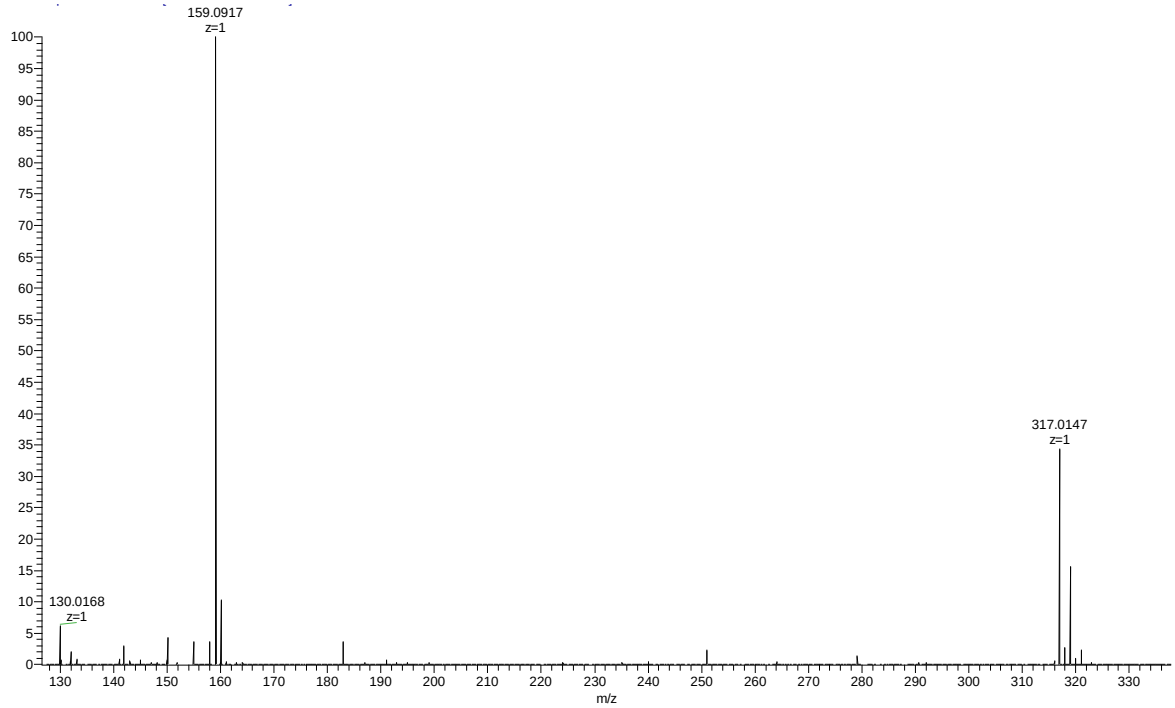

Fig 12. ESI-MS spectra of Ni**L**[5]

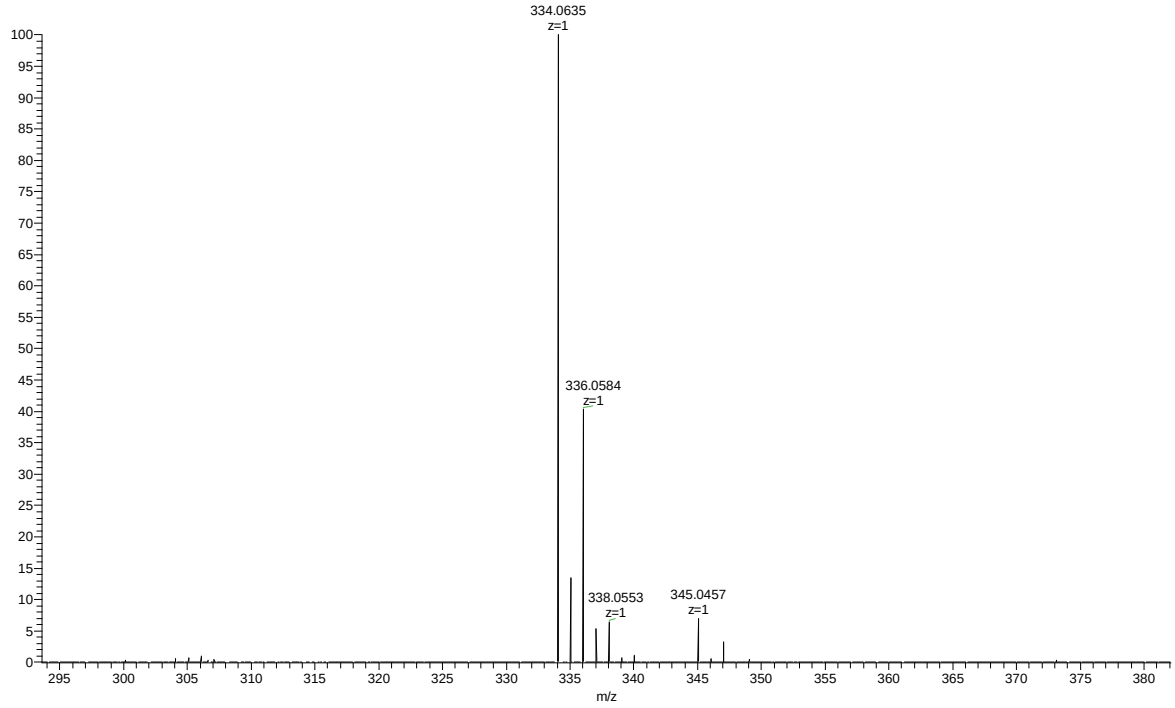

Fig 13. ESI-MS spectra of Ni**L**[7]

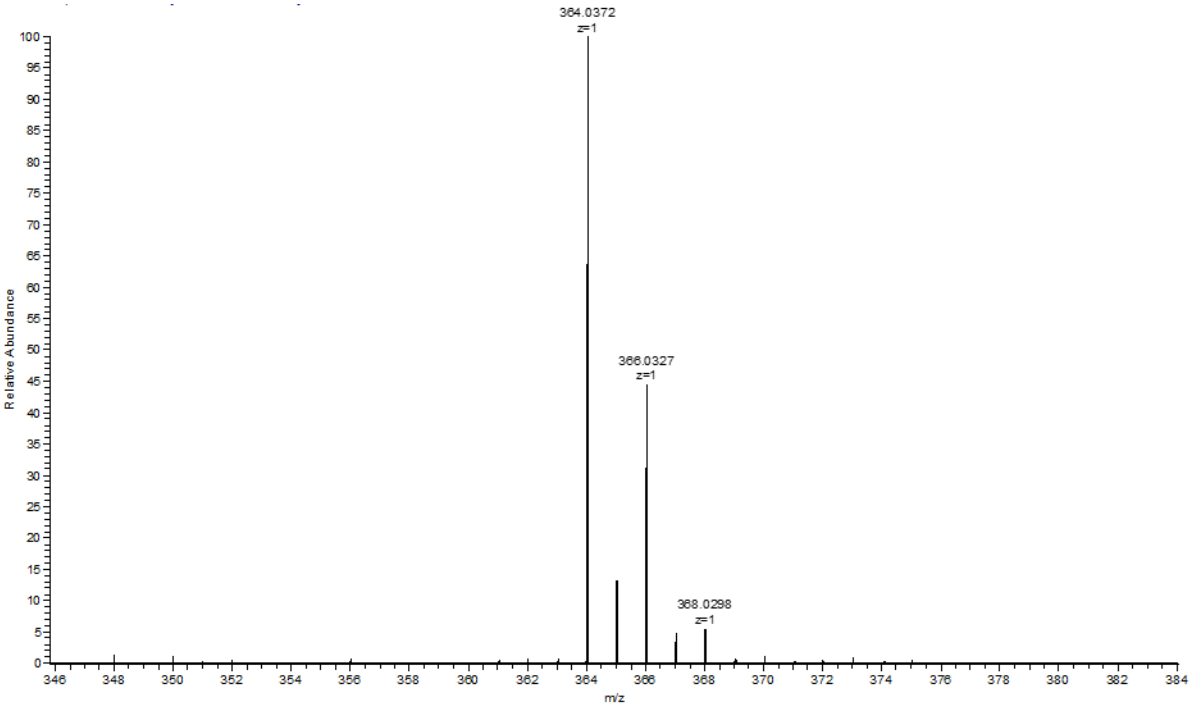

Fig 14. ESI-MS spectra of Ni**L**[8]

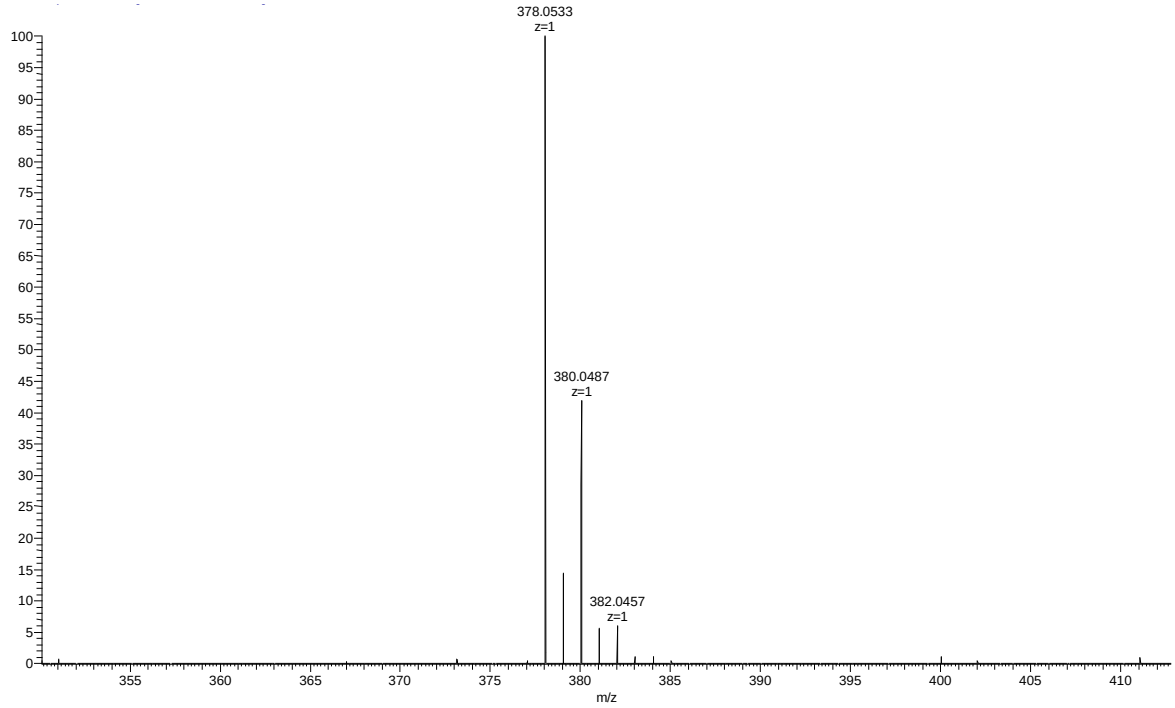

Fig 15. ESI-MS spectra of Ni**L**[10]

Appendix 2: Selected NMR spectra

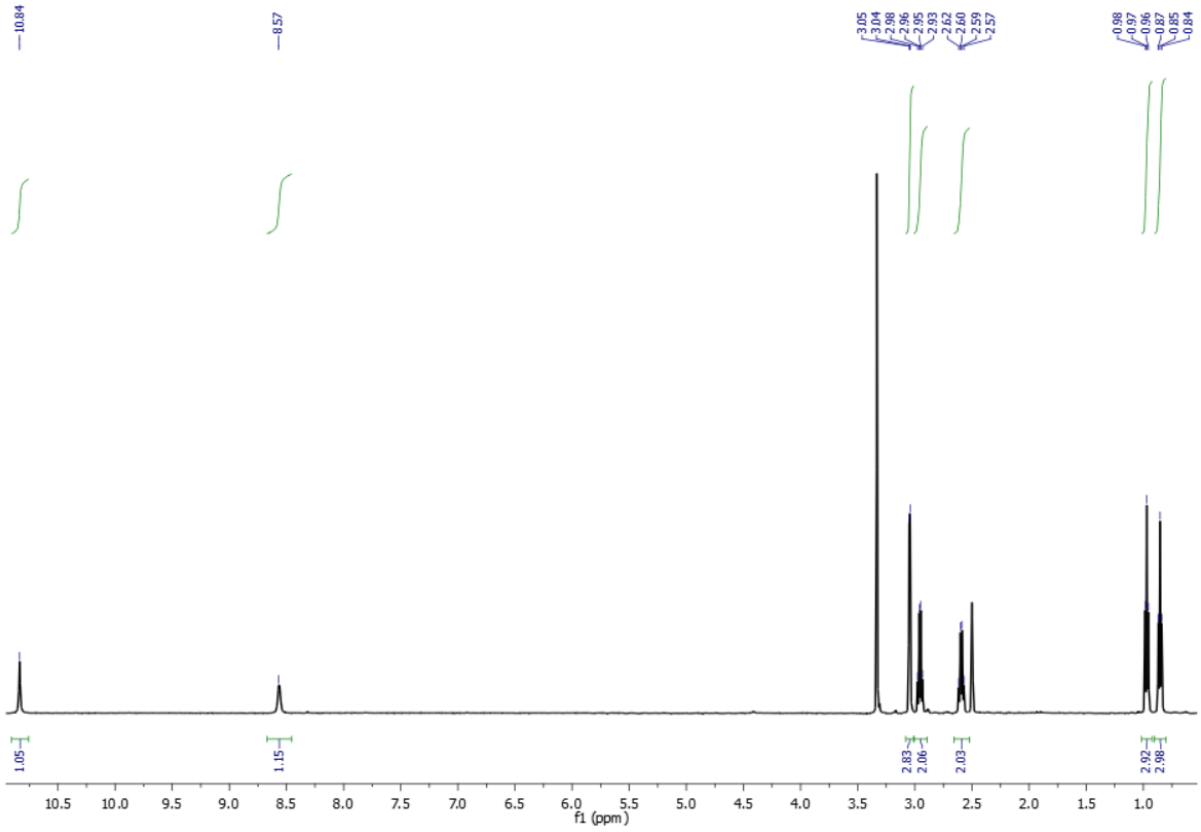

Figure 16: ^{1}H-NMR of **1** in DMSO

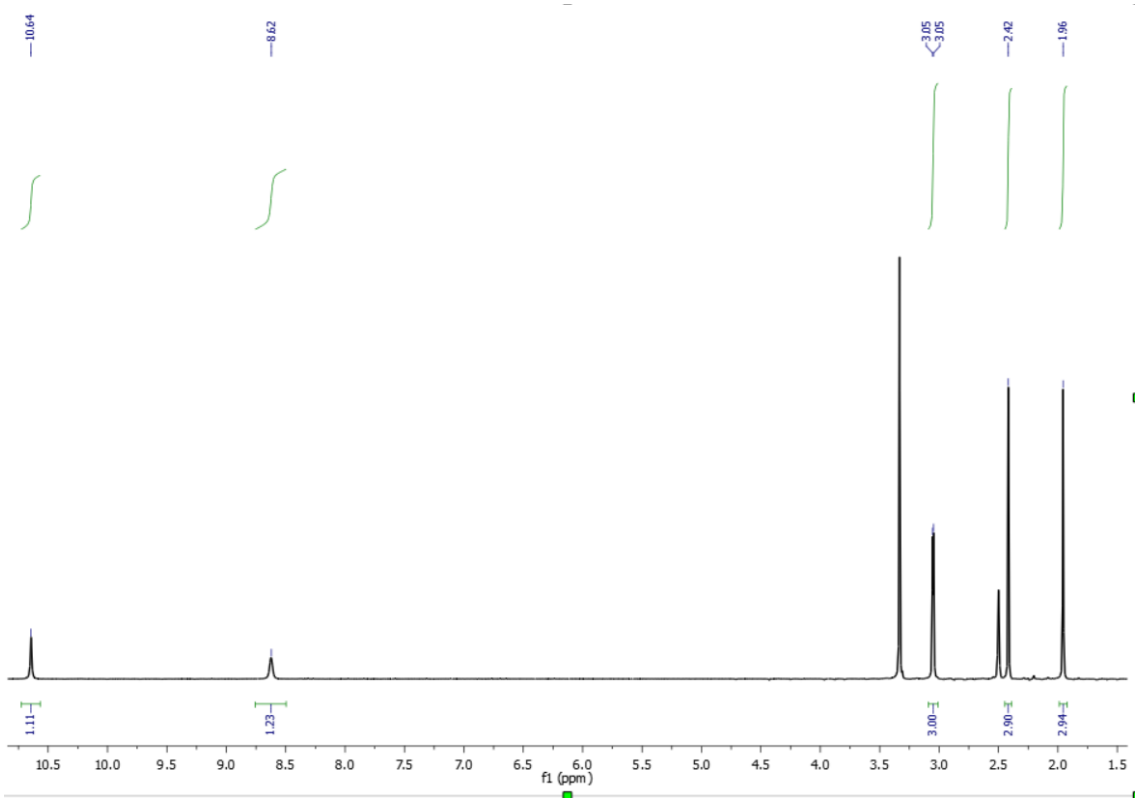

Figure 17: ^{1}H-NMR of **2** in DMSO

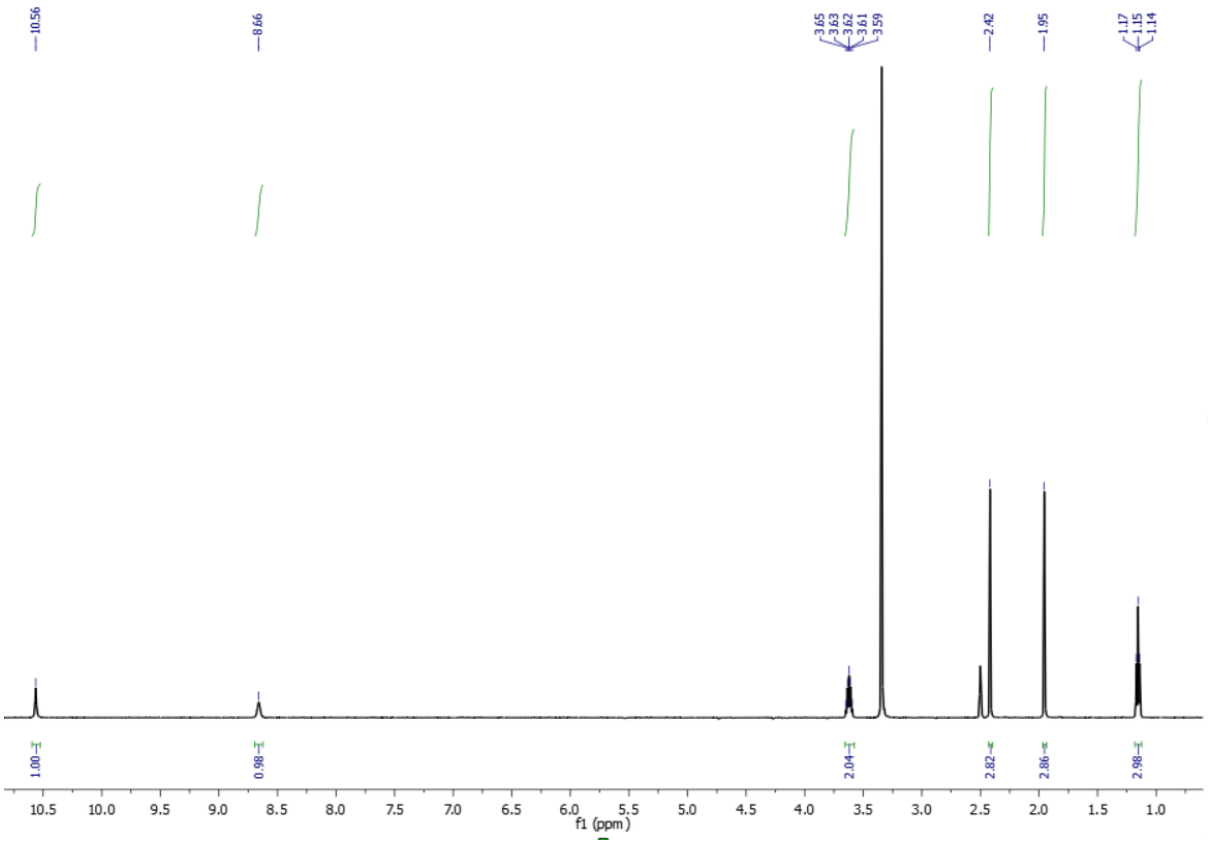

Figure 18: ^{1}H-NMR of **3** in DMSO

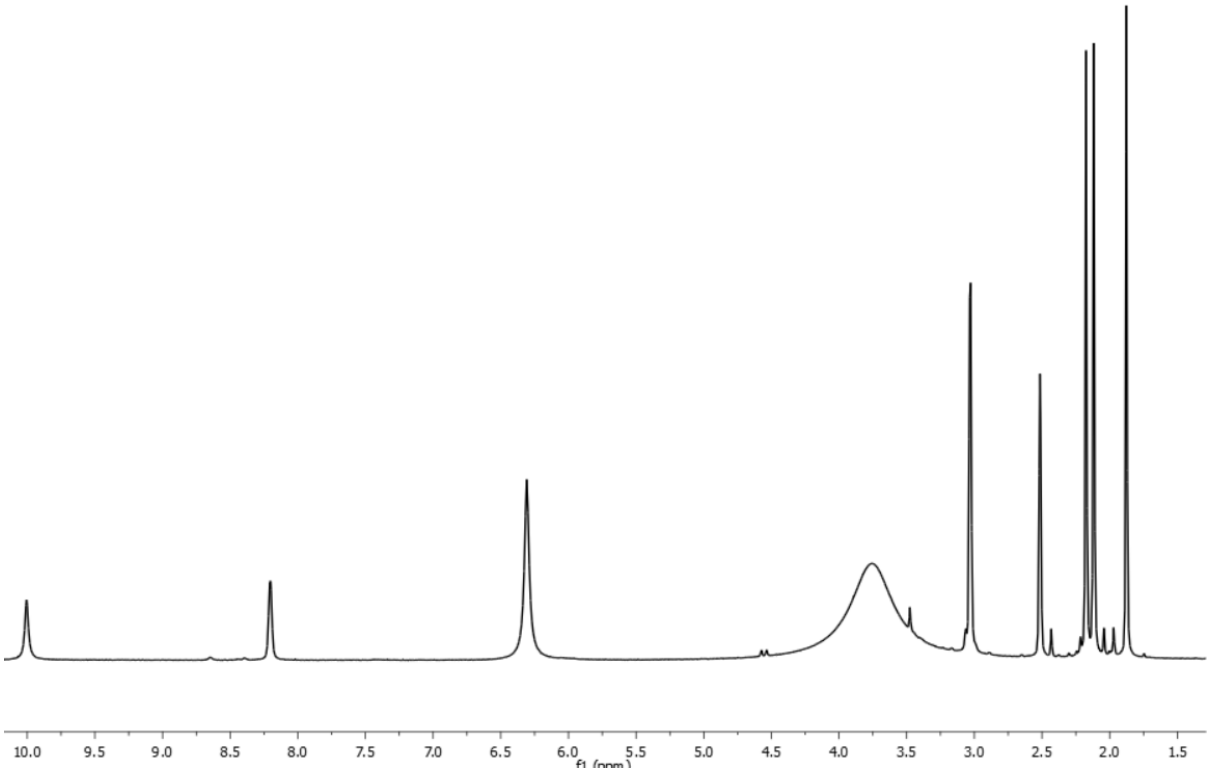

Figure 19: ^{1}H-NMR of H_2**L**^{1} in DMSO

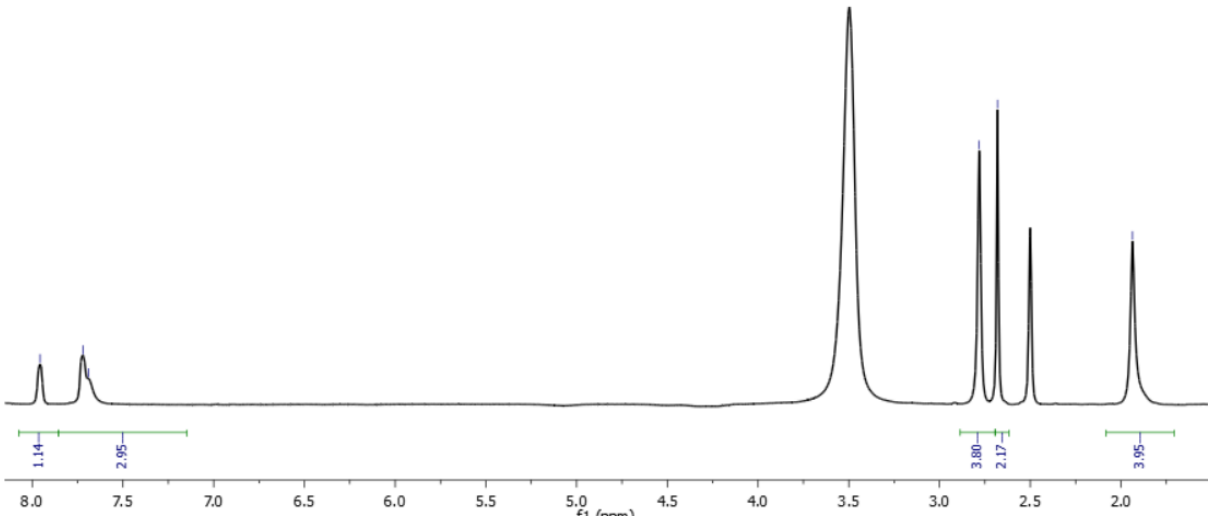

Figure 20: ^{1}H-NMR of Ni**L**^{5} in DMSO

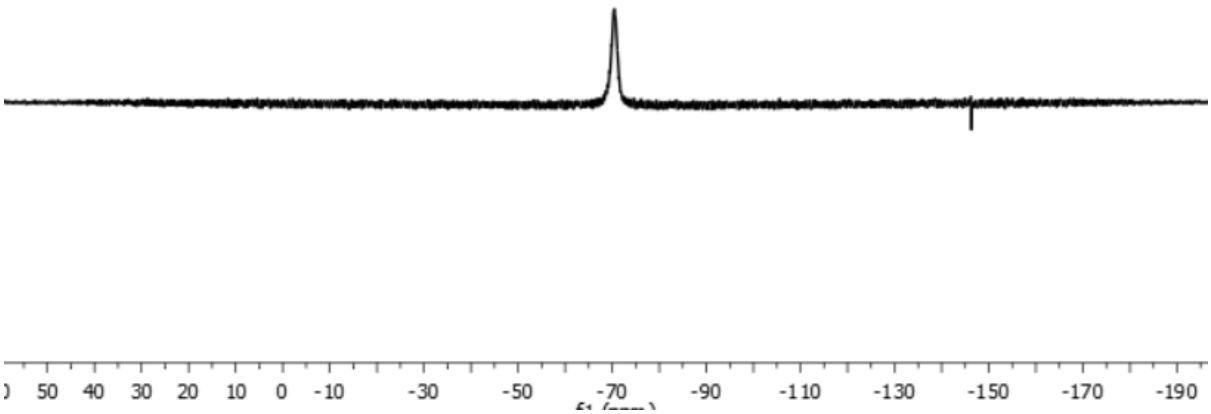

Figure 21: ^{19}F-NMR of Ni**L**^{5}

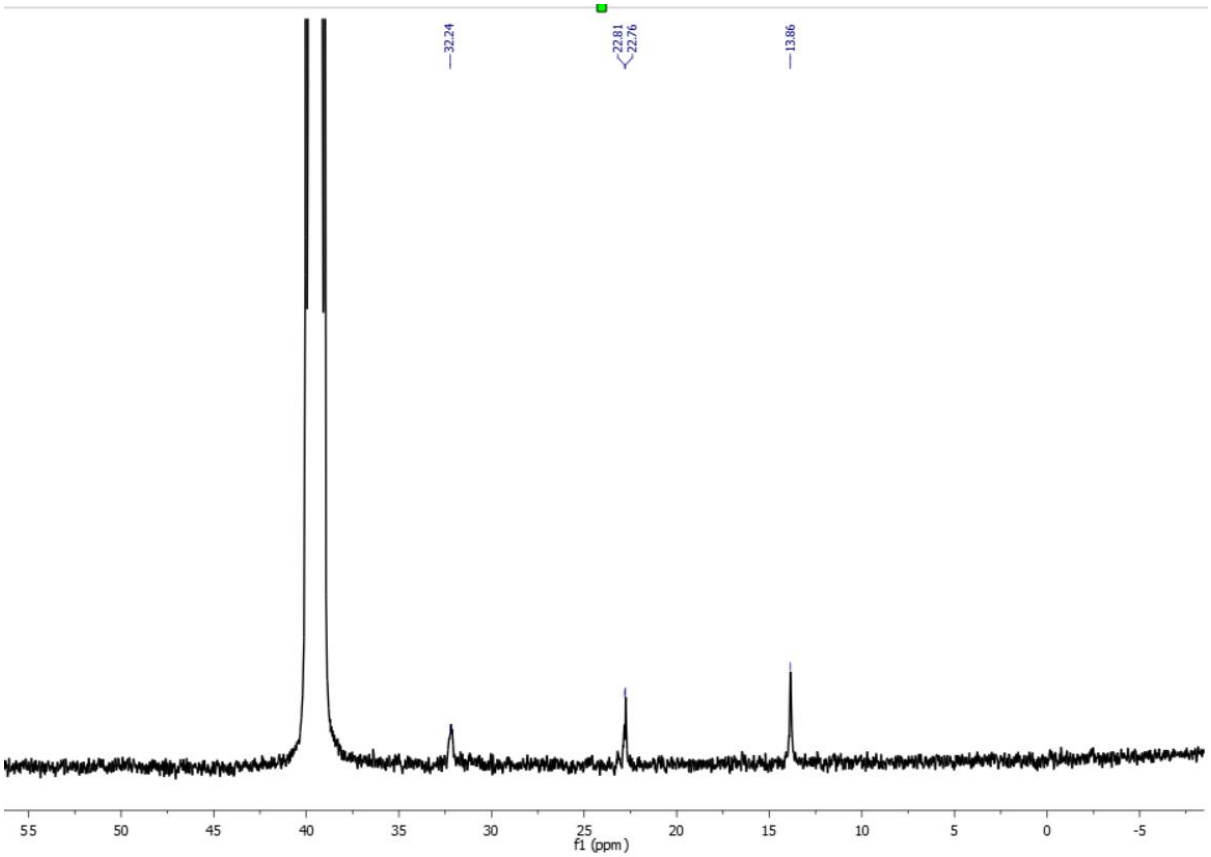

Figure 22: ^{13}C-NMR of Ni**L**^{5}

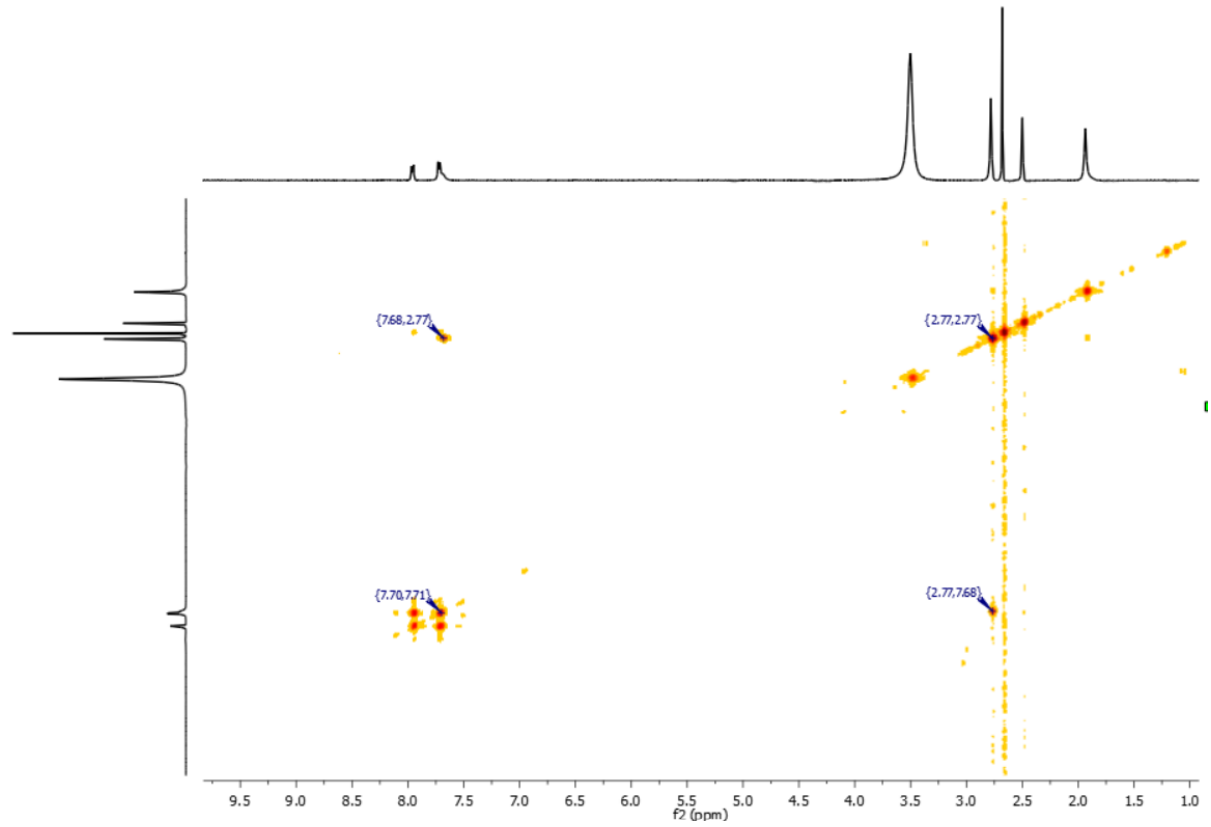

Figure 23: ^{1}H-NMR COSY of Ni**L**^{5}

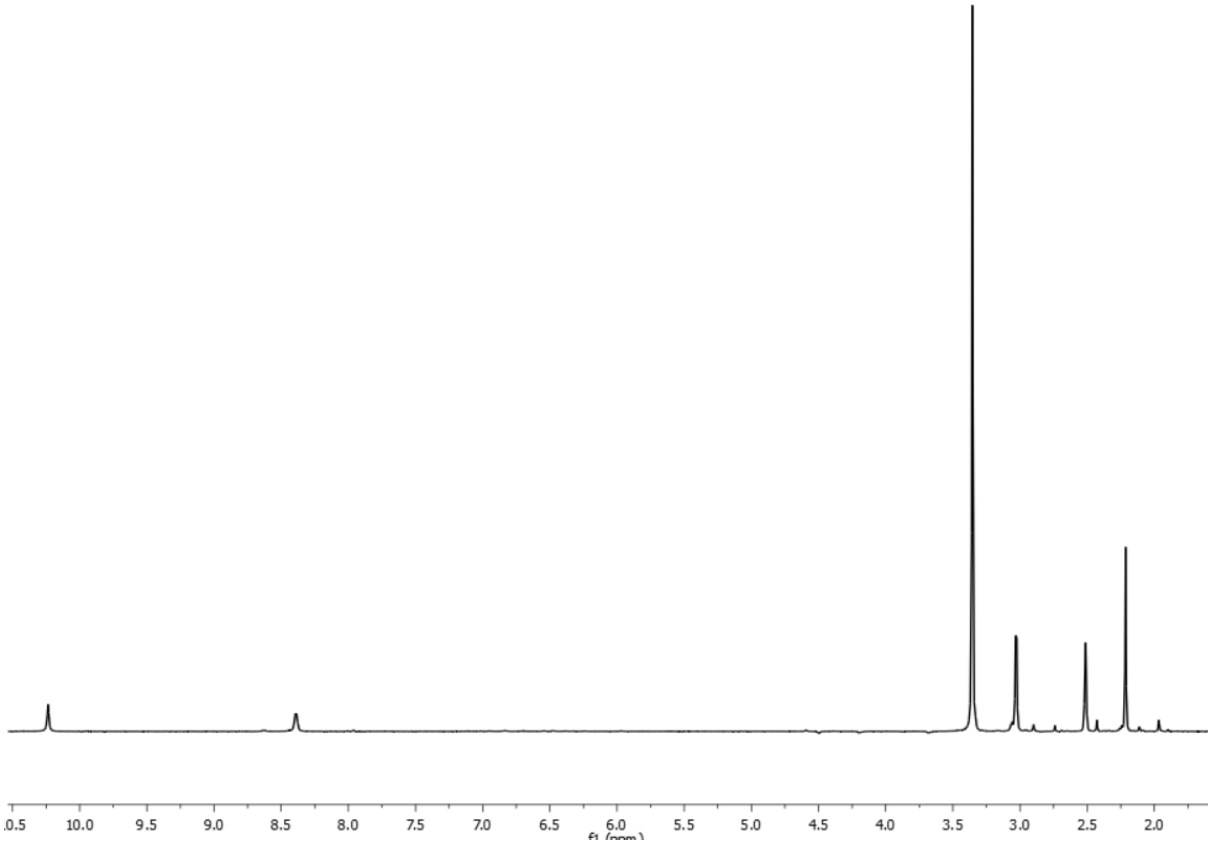

Figure 24. ^{1}H-NMR of H_2ATSM in DMSO